Investigation on Four-Wave-Mixing-Based Temporal Measurement of Low-Power-Density Optical Pulse

Bowen Ma, Lei Yu, Jianping Chen, and Weiwen Zou, *Senior Member, IEEE*

***Abstract*— We theoretically and experimentally investigate an all-optical temporal measurement of low-power-density optical pulse shape based on the four-wave-mixing process. It is found that two parameters of the pulse width ratio and frequency difference of the two optical sources are crucial to the measurement accuracy. The qualitative analysis of the impact of the two parameters on the measurement accuracy is employed by simulation. The normalized error denoting the measurement accuracy becomes worse when the pulse width ratio becomes larger, whereas it keeps relatively stable when various overlapping-free frequency differences are applied. In the experiment, temporal measurement of an actively mode-locked laser with ∼10-picosecond duration at a repetition frequency of 20.095 GHz is demonstrated, verifying the simulation analysis.**

***Index Terms*— Shape measurement, optical pulse measurements, optical mixing.**

I. Introduction

LASER pulse has been used in a wide range of scientific research fields for diverse applications, such as material processing [1], ultrafast fluorescence spectroscopy [2], biological system imaging [3], and microwave photonics processing [4]. The quality of the applied laser pulse (e.g. shape uniformity) corresponds to distinct accuracy and efficiency of all of these applications. Thus, to characterize the temporal profile of the pulse as precise as possible is increasingly meaningful and beneficial for the relative research fields. Up to date, the most widely-used techniques to characterize the optical pulse shape are based on the second-harmonic-generation (SHG) correlation [5], [6]. The frequency resolved optical-gating (FROG) has also been extensively adopted for a detailed pulse shape recovery in optical pulse shape measurement, so as to reserve the amplitude and phase of pulses [7]–[9]. Additionally, optical pulse can be measured by methods employing self-phase modulation [10], [11]. In many cases, auto-correlation-based method is an effective way to roughly determine the pulse width [12], [13]. Alternatively, the temporal shape can be obtained by the cross-correlation-based method [14], [15].

As the pulse duration descends from picosecond to shorter femtosecond, however, temporal characterization techniques intensively focus on the femtosecond magnitude. Although accurate measurement has been implemented on femtosecond pulse (e.g. by FROG), there is less investigation devoted to the picosecond pulse characterization due to its longer-delay and higher-spectral-resolution requirement. The typical pulse width for a passively mode-locked laser (PMLL) at a pulse repetition rate (PRR) of hundreds of MHz is at the order of hundreds of femtoseconds, which is one or two orders of magnitude lower than an actively mode-locked laser (AMLL) at a repetition rate of tens of GHz. As a consequence, the power-density of the AMLL pulse decreases dramatically. In such a condition, methods with a temporal resolution of tens of femtoseconds such as the SHG cross-correlation cannot help with measuring the shape of AMLL due to the low power density. This is because the low energy conversion efficiency of SHG method results in the high threshold of the detection power density, which is far beyond the power density of AMLL. Therefore, how to effectively determine the shape of low-power-density optical pulse with tens of picoseconds duration becomes a practical problem.

In this letter, we investigate the measurement accuracy of the four-wave-mixing (FWM) based temporal measurement of low-power-density optical pulse. Compared to the existing scheme applied in all-optical oscilloscope [16], the principle and architecture we adopted here are similar. What we mainly focus on is the measurement accuracy as a function of two important parameters related to the sampling and input signal, that is, pulse width ratio and frequency difference. By measuring the pulse shape of an AMLL source at 20.095 GHz, the theoretical analyses are experimentally verified.

II. Principle and Simulation

The principle of the FWM [17] based temporal measurement of low-power-density optical pulse is schematically shown in Fig. 1(a), which performs an all-optical sampling function in time domain at a wide spectrum range. Two optical pulse trains, consisting of a narrower-pulse-width one at a lower PRR of f_0 generated from a PMLL and a wider-pulse-width one at a higher PRR denoted as $Nf_0 + \delta f$ generated from an AMLL, are sent to the all-optical sampling segment. The sampled result is denoted by an envelope as a decelerating

Manuscript received October 23, 2018; revised February 15, 2019; accepted February 24, 2019. Date of publication March 4, 2019; date of current version March 27, 2019. This work was supported in part by the National Natural Science Foundation of China under Grant 61822508, Grant 61571292, and Grant 61535006. *(Corresponding author: Weiwen Zou.)*

The authors are with the State Key Laboratory of Advanced Optical Communication Systems and Networks, Department of Electronic Engineering, Shanghai Jiao Tong University, Shanghai 200240, China (e-mail: bowenma@sjtu.edu.cn; ylei3stone@sjtu.edu.cn; jpchen62@sjtu.edu.cn; wzou@sjtu.edu.cn).

Color versions of one or more of the figures in this letter are available online at http://ieeexplore.ieee.org.

Digital Object Identifier 10.1109/LPT.2019.2902723

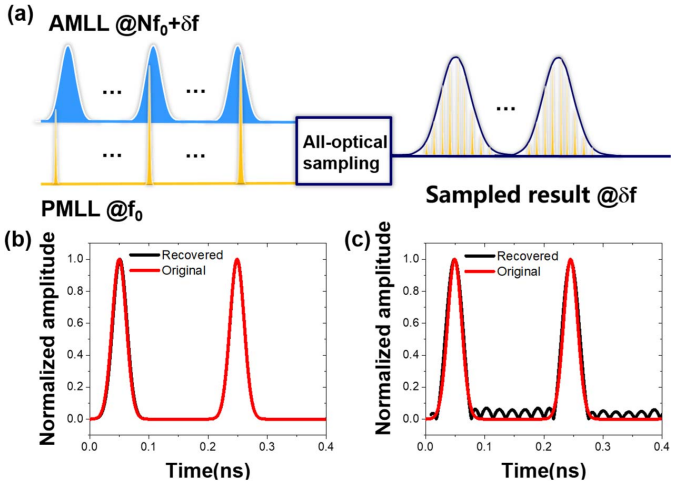

Fig. 1. Principle of the temporal shape measurement scheme and simulation of the impact on the recovered shape from δf. (a) Schematic diagram of the FWM based pulse shape measurement. (b) Simulation of ideal shape recovering with an overlapping-free δf. (c) Simulation of inferior shape recovering with an overlapping-induced δf. AMLL, actively mode-locked laser; PMLL, passively mode-locked laser.

duplication of the desired pulse shape at δf. By a narrow-band optical filter, the idle wave carrying the FWM product result is picked out. Consequently, the all-optical measurement of the low-power-density optical pulse shape is realized by low-pass filtering and scaling the time axis by a factor of $(Nf_0+\delta f)/\delta f$.

Two crucial parameters of the pulse width ratio between two pulses and the frequency difference δf have impacts on the temporal shape measurement. In Figs. 1(b) and (c), numerical simulation result qualitatively indicates that different values of δf induce distinct shape recovery accuracy. The PRRs of the two Gaussian-like optical pulse trains are set to be 5.001 GHz and 50 MHz respectively. Besides, the pulse width is 20 ps for high PRR pulse and 15 ps for low PRR pulse, which are comparable to the experimental parameters demonstrated below. After multiplication in time domain and filtering in frequency domain, a recovery factor of 5001 is applied. As shown in Fig. 1(b), the moderate frequency difference δf of 1 MHz makes the optically-sampled result overlapping-free in frequency domain. Accordingly, a complete low-frequency component separated from other components can be filtered out which in time domain is an ideal recovered pulse shape. If the PRR of high-speed pulse train is changed to 5.005 GHz, a recovery factor of 1001 and a larger frequency difference δf of 5 MHz induce the overlapped output frequency spectrum. The pulse shape recovery degrades as shown qualitatively by the ripples in Fig. 1(c). Meanwhile, the bandwidth of the desired low-frequency component depends on the value of δf.

Furthermore, we theoretically investigate the effect of the two crucial parameters on the shape measurement accuracy. Defined as the ratio of full-width-half-maximum (FWHM) of two optical pulse trains, pulse width ratio can characterize how sharp the low PRR pulse is in time domain compared to the high PRR pulse. Besides, after scaling in time domain, the figure of merit of the recovered result is evaluated via the normalized error, which is the normalized sum of the square of the difference in amplitude between the original pulse and

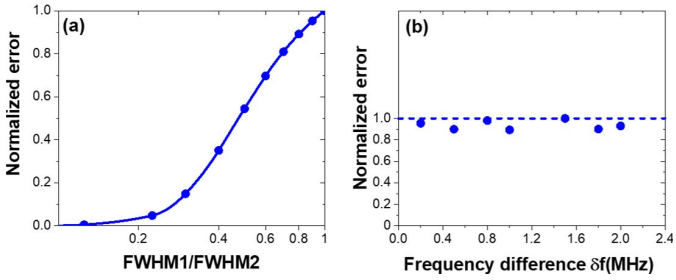

Fig. 2. Simulation of pulse width ratio (a) and overlapping-free frequency difference (b) versus the normalized error. FWHM, full-width-half-maximum; δf, frequency difference.

recovered pulse and described by:

$$e_{norm} = \left(\int (a_{ori}(t) - a_{rec}(t))^2 dt\right)/e_{max} \tag{1}$$

where e_{max} is the maximum error, and e_{norm} indicates the normalized error. The a_{ori} or a_{rec} corresponds to the amplitude of the original pulse or recovered pulse, respectively. The normalized error of the result in Fig. 1(b) is 0.08 which is significantly less than that being 1 in Fig. 1(c). It indicates that different values of frequency difference and pulse width ratio distinctly influence the normalized error.

To quantitatively verify the analyses, we simulate two pulse trains with the PRR of 0.251 GHz and 50 MHz and assume the pulse shape to be Gaussian-like. The pulse trains are multiplied in time domain as a function of the FWM effect. Here, we ignore the dispersion and loss in the fiber link for simplicity. The recovered pulse is obtained by filtering the sampled result with a low-pass filter and scaling the time axis with the recovery factor of $(Nf_0 + \delta f)/\delta f$. By setting up different pulse widths of low PRR pulse from 1.5 ps to 20 ps and keeping the pulse width of high PRR pulse constant to be 20 ps, the pulse width ratio changes from 0.075 to 1, then we derive the normalized error. The δf remains a constant of 1 MHz. As depicted in Fig. 2(a), it shows that the bigger the difference between two pulse widths is, the recovered result suffers the less error. That is to say, as the low PRR optical pulse becomes sharper, the output of all-optical sampling becomes more accurate, which brings the better recovery accuracy. On the other hand, we keep the pulse width ratio unchanged at 0.075 and analyze different overlapping-free δf values, which is depicted in Fig. 2(b). Without the appearance of overlapping in frequency domain as mentioned above, one can find that the normalized errors are at the same level, which means there is a tiny impact on the normalized error induced by the frequency difference. Variation of δf only induces different bandwidths of the recovered pulse in frequency domain. Therefore, when setting the value of δf in the experiment, only if there is no overlapping in frequency domain, it is optional to change δf value for matching different bandwidths of back-end low-pass filters.

III. Experiment Results and Discussion

The experimental setup for the low-power-density optical pulse shape measurement of an AMLL is shown in Fig. 3. An optical pulse train output from a PMLL (Menlo Systems,

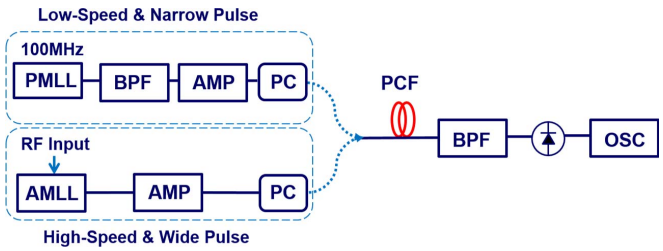

Fig. 3. Experiment setup for temporal shape measurement of an AMLL. BPF, band-pass filter; AMP, optical amplifier; PC, polarization controller; PCF, photonic crystal fiber; OSC, oscilloscope.

LAC-1550) at the PRR of 100 MHz, playing the role of detection pulse, is sent to a band-pass filter (BPF) (Alnair Labs, CVF-300CL) and an optical amplifier (Calmar, AMP-ST22) which filters out the main spectral components of PMLL centering at 1560 nm (bandwidth, 0.6 nm) and enables them sufficient optical power (∼18 dBm) to generate the FWM effect. The bandwidth of the BPF is determined to avoid the overlapping of optical spectrum of the two sources and to make the efficiency of the FWM effect as high as possible. As a result, the pulse width of PMLL is broadened to be ∼10 ps after filtering. Besides, a polarization controller (PC) is applied to improve the efficiency of polarization-dependent FWM process. In the other branch of Fig. 3, a radio frequency (RF) signal from a signal generator (Keysight, E8257D) serves as the input to an AMLL source (Calmar, PSL-10-TT) at 20.095 GHz with δf of 5 MHz. An optical amplifier (Calmar, AMP-ST30) and a PC are added as well. The optical power in this branch before coupler is approximately 18 dBm. Next, two optical pulse trains are coupled to a photonic crystal fiber (PCF) (Crystal Fiber A/S, NL-1550-NEG-1) as a high-nonlinear-coefficient medium [18] where the FWM takes place. After that, the idle wave is selected by a BPF (Alnair Labs, CVF-220CL) and converted to an electric signal by a photodetector (PD, DC-300 MHz). At the end, a digital oscilloscope (OSC) (Keysight, DSO-S 804A) laid after three types of electric low-pass filters (Mini-circuits, SLP-21.4+, SLP-10.7+, SLP-50+) acquires the recovered shape at a sampling rate of 1 GSa/s.

Two groups of experiments are carried out to study the impacts on the shape measurement performance from the two crucial parameters. From the label on the front panel of the AMLL, we can get the reference value of the output pulse width. In the first group, we hold the frequency difference δf as a constant of 5 MHz and choose four output pulse widths of the AMLL corresponding to different pulse width ratios. The results of the first group of experiments are illustrated in Fig. 4. As an instance of the results shown in Fig. 4(a), the recovered pulse and an ideal Gaussian pulse as reference are presented. The recovered pulse width of 16.83 ps is greater than the reference one of 13 ps, which is due to the dispersion in the optical link of the experimental setup. The dispersion can be evaluated by the difference between the recovered and reference pulse widths. Since the length of the FWM process and its dispersion coefficient keeps maintained, the evaluated dispersion should be proportional to the optical spectral width $\delta\lambda$ of AMLL's optical pulse, which matches

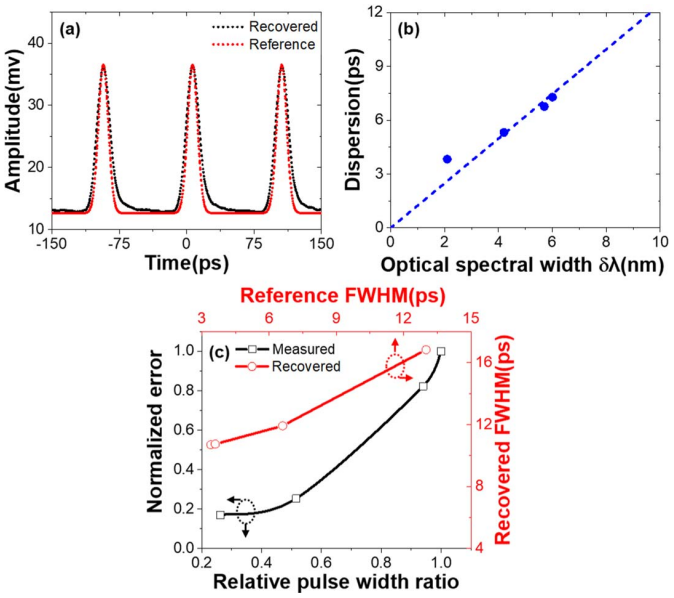

Fig. 4. Temporal shape measurement results with variant pulse width ratio and invariant frequency difference δf. (a) Recovered pulse shape with a FWHM of 16.83 ps and Gaussian-like reference with a FWHM of 13 ps. (b) Dispersion of the recovered pulse versus the optical spectral width of the AMLL. (c) Cycles: comparison of reference pulse width and recovered pulse width. Squares: normalized errors when different pulse width ratios are applied. FWHM, full-width-half-maximum.

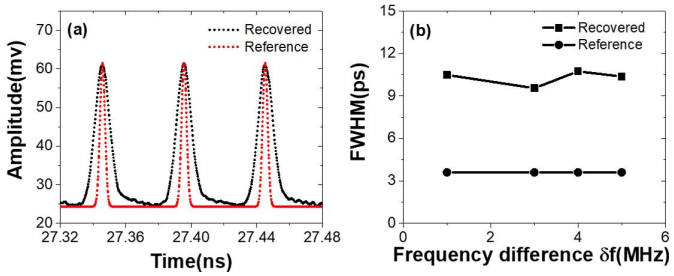

Fig. 5. Experimental results with variant frequency difference δf and invariant pulse width ratio. (a) Recovered pulse shape with a FWHM of 10.37 ps and Gaussian-like reference with a FWHM of 3.6 ps. (b) Recovered pulse width in the condition of applying various frequency difference δf versus the constant reference pulse width. FWHM, full-width-half-maximum.

well the experimental results indicated by Fig. 4(b). Note that the slope of the evaluated linearity between optical spectral width and dispersion can offer a modification method to the other pulse shape width so as to get a better measurement accuracy. In Fig. 4(c), cycles represent that when increasing the output pulse width with a constant δf, the recovered pulse width increases as well. Additionally, when the AMLL pulse width changes, the relative pulse width ratio is variant. Squares indicate the relationship between the relative pulse width ratio and the normalized error. It is found that the normalized error decreases along with the decrease of the relative pulse width ratio. This phenomenon is consistent with the simulation analyses in Fig. 2(a). More shaper the sampling signal is, more accurate the recovered result becomes.

Second, we set four frequency difference values when keeping the output pulse width at a fixed value of 3.6 ps. Note that overlapping-free condition in frequency domain has been guaranteed. The experimental results are illustrated

in Fig. 5. An example of the recovered pulse compared with the Gaussian reference pulse is depicted in Fig. 5(a). The FWHM of the recovered pulse is 10.37 ps. The difference of the pulse widths between the two pulses is obvious, which is mainly owing to the dispersion described in Fig. 4(b). In Fig. 5(b), the recovered pulse width and its corresponding reference value at four frequency difference values are depicted. The recovered pulse widths keep unchanged at the level of ∼10 ps. Variant frequency difference has no effect on the recovered pulse width. This experimental result is in agreement with the simulation analyses in Fig. 2(b).

IV. Conclusion

In summary, the all-optical-sampling based scheme of pulse shape measurement for low-power-density optical pulse has been investigated. The impact of two vital parameters on the measurement accuracy is analyzed by simulation and validated by experiment. The theoretical and experimental results are consistent. The normalized error grows up as the pulse width ratio increases and keeps unchanged as the overlapping-free frequency difference changes. In the experiment, optical pulse shape of an AMLL at 20.095 GHz is measured. The width of the recovered pulse is relatively greater than that of the reference pulse. Dispersion is a cause of this phenomenon which can be modified in the results to get a better measurement performance. Future work will be mostly about the improvement of the measurement accuracy for low-power-density optical pulse.

References

[1] M. Malinauskas, P. Danilevičius, and S. Juodkazis, "Three-dimensional micro-/nano-structuring via direct write polymerization with picosecond laser pulses," *Opt. Express*, vol. 19, no. 6, pp. 5602–5610, Mar. 2011.

[2] Y. Pu, W. Wang, R. B. Dorshow, B. B. Das, and R. R. Alfano, "Review of ultrafast fluorescence polarization spectroscopy [Invited]," *Appl. Opt.*, vol. 52, no. 5, pp. 917–929, Feb. 2013.

[3] R. Kawakami *et al.*, "Visualizing hippocampal neurons with *in vivo* two-photon microscopy using a 1030 nm picosecond pulse laser," *Sci. Rep.*, vol. 3, Jan. 2013, Art. no. 1014.

[4] G. Yang, W. Zou, L. Yu, and J. Chen, "Influence of the sampling clock pulse shape mismatch on channel-interleaved photonic analog-to-digital conversion," *Opt. Lett.*, vol. 43, no. 15, pp. 3530–3533, Aug. 2018.

[5] I. Walmsley and C. Dorrer, "Characterization of ultrashort electromagnetic pulses," *Adv. Opt. Photon.*, vol. 1, no. 2, pp. 308–437, Apr. 2009.

[6] B. Alonso *et al.*, "Spatiotemporal amplitude-and-phase reconstruction by Fourier-transform of interference spectra of high-complex-beams," *J. Opt. Soc. Amer. B, Opt. Phys.*, vol. 27, no. 5, pp. 933–940, May 2010.

[7] R. Trebino, *Frequency-Resolved Optical Gating: The Measurement of Ultrashort Laser Pulses*. Boston, MA, USA: Springer, 2000.

[8] X. Li, W. Zou, and J. Chen, "41.9 fs hybridly mode-locked Er-doped fiber laser at 212 MHz repetition rate," *Opt. Lett.*, vol. 39, no. 6, pp. 1553–1556, Mar. 2014.

[9] X. Li, W. Zou, K. Wu, and J. Chen, "Timing-jitter reduction by use of a spectral filter in a broadband femtosecond fiber laser," *IEEE Photon. Technol. Lett.*, vol. 27, no. 8, pp. 911–914, Apr. 15, 2015.

[10] E. A. Anashkina, A. V. Andrianov, M. Y. Koptev, and A. V. Kim, "Complete field characterization of ultrashort pulses in fiber photonics," *IEEE J. Sel. Topics Quantum Electron.*, vol. 24, no. 3, May/Jun. 2018, Art. no. 8700107.

[11] K. Baudin, F. Audo, and C. Finot, "Fiber-based measurement of temporal intensity and phase profiles of an optical telecommunication pulse through self-phase modulation," *Microw. Opt. Techn. Lett.*, vol. 60, no. 4, pp. 882–886, Mar. 2018.

[12] P. Yeh, "Autocorrelation of ultrashort optical pulses using polarization interferometry," *Opt. Lett.*, vol. 8, no. 6, pp. 330–332, Jun. 1983.

[13] K. L. Sala, G. Kenney-Wallace, and G. E. Hall, "CW autocorrelation measurements of picosecond laser pulses," *IEEE J. Quantum Electron.*, vol. QE-16, no. 9, pp. 990–996, Sep. 1980.

[14] G. Priebe, K. A. Janulewicz, V. I. Redkorechev, J. Tümmler, and P. V. Nickles, "Pulse shape measurement by a non-collinear third-order correlation technique," *Opt. Commun.*, vol. 259, no. 2, pp. 848–851, Mar. 2006.

[15] Y. Wang *et al.*, "Single-shot measurement of $>10^{10}$ pulse contrast for ultra-high peak-power lasers," *Sci. Rep.*, vol. 4, Jan. 2014, Art. no. 3818.

[16] T. Kiatchanog, K. Igarashi, T. Tanemura, D. Wang, K. Katoh, and K. Kikuchi, "Real-time all-optical waveform sampling using a passively mode-locked fiber laser as the sampling pulse source," in *Proc. Opt. Fiber Commun. Conf. Nat. Fiber Opt. Eng. Conf.*, Mar. 2006, pp. 1–3, Paper OWN1.

[17] G. Agrawal, *Nonlinear Fiber Optics*, 5th ed. Salt Lake City, UT, USA: Academic, 2013.

[18] W. Zou, Z. He, and K. Hotate, "Experimental investigation on Brillouin scattering property in highly nonlinear photonic crystal fiber with hybrid core," *Opt. Express*, vol. 20, no. 10, pp. 11083–11090, May 2012.